Nanoscale Advances

ROYAL SOCIETY OF CHEMISTRY

PAPER

View Article Online
View Journal | View Issue

Cite this: *Nanoscale Adv.*, 2020, **2**, 4604

CdS crown growth on CdSe nanoplatelets: core shape matters†

Anja Schlosser, [ab] Rebecca T. Graf[ab] and Nadja C. Bigall [*abc]

Received 29th July 2020
Accepted 1st September 2020

DOI: 10.1039/d0na00619j

rsc.li/nanoscale-advances

Cadmium chalcogenide nanoplatelets (NPLs) have gained tremendous attention in the past decade due to their extremely narrow optical features and their special electronic properties. For the application of the NPLs as optical emitters, in (photo) catalysis or sensing, further modification of the pristine (core) NPLs can be required. Therefore, many procedures for the synthesis of crowns (lateral extension of the core NPLs), shells and particle domains on the NPLs have already been developed. CdSe/CdS core/crown NPLs are characterised by extremely short photoluminescence (PL) lifetimes and high PL quantum yields (PLQYs) and might therefore be ideal candidates for lighting applications. In this work, we show how the optical properties of CdSe/CdS core/crown NPLs, especially their PLQYs, can be strongly improved by applying a sulphur precursor with a low reactivity. Under optimised conditions, the new procedure allows the growth of uniform CdS crowns around CdSe core NPLs with various lateral sizes, thicknesses and shapes. In addition, the modified growth kinetics was investigated by various methods, including UV/vis and PL spectroscopy as well as transmission electron microscopy.

1 Introduction

Since the first report on the wet-chemical synthesis of free-standing CdSe nanoplatelets (NPLs) more than a decade ago, great effort was invested into the understanding and manipulation of their optical and electronic properties.[1,2] This type of colloidally dispersed NPLs is in general characterised by lateral dimensions which are clearly exceeding the bulk exciton Bohr radius of the respective material, while their thickness can be controlled in the order of a few atomic layers (so-called monolayers, MLs). The described structural characteristics lead to a strong one-dimensional quantum confinement in the thickness direction, hence very narrow emission spectra with specific emission wavelengths as well as high absorption cross-sections and very short radiative lifetimes due to the presence of a giant oscillator strength transition (GOST) are observed.[1,3,4] Due to these and other exceptional optical and electronic properties, cadmium chalcogenide NPLs have already been applied in the construction of various devices such as lasers,[5–8] sensors,[9,10] light-emitting diodes (LEDs)[11–16] displays,[17] and phototransistors.[18]

However, for most of the listed applications a further modification of the pristine core-only NPLs was required in order to manipulate *e.g.* their emission colour or chemical stability. To date, a manifold of ways to modify the NPL structure has already been developed, including the growth of shells, crowns and domains around the core NPLs.[19] Depending on the desired application, the modification material can either be a semiconductor (wide or narrow bandgap)[20–24] or a metal.[25,26] If a shell is grown around a core NPL, the shell material is deposited on all surfaces of the NPL, which results in a lateral extension as well as in an increase in the NPL thickness. This, in turn, leads to a good surface passivation, thus enhanced photoluminescence quantum yields (PLQYs) and chemical stabilities but also to bathochromically shifted emission features independent of the actual band structures due to the weakening of the quantum confinement.[23,27–30] So-called core/crown structures, in contrast, are obtained by the lateral extension of the core NPLs with the crown material while retaining the core thickness. The optical properties of these heterostructures, however, strongly depend on the band positions of the applied crown material, ranging from nearly unaltered emission wavelengths for CdSe/CdS core/crown NPLs to strong bathochromic emission shifts and even the appearance of dual wavelength emission for CdSe/CdTe and CdSe/$CdSe_{1-x}CdTe_x$ core/crown NPLs, respectively.[21,22,31,32] In most cases, the crown growth also involves a great improvement of the PLQY due to the passivation of the comparatively defect-rich edge facets of the NPLs.[33,34]

In order to further enhance the PLQY of core/crown NPLs or core/shell nanocrystals (NCs) in general, the interface between

[a]*Institute of Physical Chemistry and Electrochemistry, Leibniz Universität Hannover, 30167 Hannover, Germany. E-mail: nadja.bigall@pci.uni-hannover.de*

[b]*Laboratory of Nano and Quantum Engineering, Leibniz Universität Hannover, 30167 Hannover, Germany*

[c]*Cluster of Excellence PhoenixD (Photonics, Optics, and Engineering Innovation Across Disciplines), 30167 Hannover, Germany*

† Electronic supplementary information (ESI) available: Characterisation of the core NPLs, details on the approximation of the CdS crown area, further structural and optical characterisation of core/crown NPLs. See DOI: 10.1039/d0na00619j

core and shell needs to be optimised. Several approaches to tackle this issue have already been reported for core/shell NPLs, quantum dots (QDs) or nano rods, including high-temperature shell growth,[16,23,28,30] the introduction of post-synthetic annealing steps[35] and the utilisation of low-reactivity shell precursors to slow down the growth rate.[36] To the synthesis of highly luminescent core/crown NPLs the latter way is particularly applicable, as core-only NPLs are comparatively temperature-sensitive and as higher temperatures could moreover promote the three-dimensional shell growth.

In order to optimise the optical properties and uniformity of CdSe/CdS core/crown NPLs we applied tri-*n*-octylphosphine-sulphur (TOPS) as a low-reactivity sulphur precursor for the CdS crown growth and examined its effects on the optical properties of the synthesised heterostructures. TOPS has already been widely applied as a sulphur precursor in the synthesis of metal sulfide shells on NCs of various shapes and material compositions,[37–40] but so far not in the synthesis of CdS crowns on CdSe NPLs. We show that by the addition of TOP the CdS crown growth rate can be remarkably decreased so that core/crown NPLs with more uniform crowns and higher PLQYs (up to 90%) are obtained, independent of the CdSe core geometry, size and thickness. Due to the modified sulphur precursor, the presented reaction procedure yields NPL solutions of a high colloidal stability and was moreover observed to be very reproducible and easily up-scalable enabling the production of large amounts of core/crown NPLs for possible lighting applications. Finally, we demonstrate that by simply adjusting the injection rate of the S precursor the solely 2D crown growth can be transformed into 3D CdS growth, yielding CdSe/CdS core/crown NPLs with an increased crown thickness and bathochromically shifted PL emission.

2 Experimental

2.1 Chemicals

Sodium myristate (≥99%), methanol (MeOH, ≥99.8%), 1-octadecene (ODE, 90%), sulphur (99.98%), *n*-hexane (≥99%) and ethanol (EtOH, ≥99.8%) were purchased from Sigma Aldrich. Cadmium nitrate tetrahydrate (99.999%), selenium (99.999%, 200 mesh) and oleic acid (OlA, 90%) were supplied by Alfa Aesar. Cadmium acetate dihydrate [$Cd(Ac)_2$, 98%], tellurium (99.999%, 60 mesh) and tri-*n*-octylphosphine (TOP, 97%) were purchased from ABCR. All chemicals except ODE were used as received without further purification. ODE applied for the preparation of the chalcogenide precursor solutions was obtained by degassing at 120 °C in vacuum ($p \leq 1 \times 10^{-3}$ mbar) for at least 6 h. Afterwards, the purified ODE was stored in an air-free glove box.

2.2 Synthesis procedures

2.2.1 Preparation of cadmium myristate. Cadmium myristate applied for the synthesis of CdSe core NPLs was prepared according to a literature procedure.[21]

2.2.2 Preparation of chalcogenide precursor solutions. 1 M TOPS and TOPSe solutions were prepared by dispersing 160.3 mg or 394.8 mg of sulphur or selenium, respectively, in 5 mL of TOP. To ensure complete dissolution, the solutions were stirred over night in an air-free glove box.

To prepare a 1 M TOPTe solution, 638.0 mg of tellurium powder were loaded into a 25 mL three-neck flask and the pressure in the flask was reduced below 1×10^{-3} mbar three times. Under an Ar atmosphere, 5 mL of TOP were added with a syringe and the mixture was heated to 275 °C until a clear orange solution was obtained. The TOPTe solution was allowed to cool to room temperature and stored in an air-free glove box for further use.

A 0.05 M S/ODE dispersion was prepared by mixing 11.2 mg of sulphur with 7 mL of ODE. Afterwards, the dispersion was ultrasonicated for at least 30 min until a slightly turbid solution without visible precipitate was obtained. During the ultrasonication process, the dispersion was shaken vigorously several times.

2.2.3 Synthesis of CdSe core NPLs. Quasi-rectangular and quasi-quadratic core CdSe NPLs with a thickness of 4 MLs were synthesised according to literature procedures.[10,22,41,42]

5 ML thick quasi-rectangular core NPLs were synthesised following a procedure by Naskar *et al.*[25]

Quasi-rectangular 4 ML NPLs with larger lateral dimensions were synthesised according to a literature procedure[32] with slight modifications. Briefly, 96 mg of $Cd(Ac)_2$, 180 μL of OlA and 1.075 μL of a CdSe NPL solution in hexane (quasi-rectangular core NPLs, $c_{Cd} = 50.7$ mM, $\beta_{CdSe} = 9.70$ mg mL^{-1}) were combined with 8 mL of ODE in a 25 mL three-neck flask. The hexane was removed carefully at the Schlenk line and the mixture was further degassed in vacuum at 60 °C for at least 1 h. Subsequently, the temperature was increased to 215 °C under an Ar atmosphere and 2 mL of a TOPSe/ODE solution (50 μL of a 1 M TOPSe solution mixed with 1.95 mL of ODE) were injected at a rate of 8 mL h^{-1}. After cooling down to room temperature, 15 mL of a 2 : 1 mixture of ethanol and hexane were added and the mixture was centrifuged at 4226 rcf for 10 min. Afterwards, the colourless supernatant was discarded and the NPLs were re-dispersed in 2 mL of hexane.

2.2.4 Synthesis of core/crown NPLs. CdX (X = S, Se, Te) crowns on CdSe core NPLs were obtained by following a slightly modified procedure for CdTe crown growth on CdSe NPLs.[32] At first, 8 mL of ODE, 180 μL of OlA, 96 mg of $Cd(Ac)_2$ and 1.165 mL of the core CdSe NPLs in hexane ($c_{Cd} = 40.0$ mM, $\beta_{CdSe} = 7.64$ mg mL^{-1}) were combined in a 25 mL three-neck flask. The hexane was carefully removed in vacuum at room temperature and the mixture was further degassed in vacuum for at least 1.5 h at 60 °C. Subsequently, the solution was heated to 240 °C under an Ar atmosphere. When a temperature of 215 °C was reached, 6 mL of a 0.05 M chalcogenide precursor solution in ODE was injected at a rate between 6 mL h^{-1} and 36 mL h^{-1}. To monitor the crown growth progress, aliquots (250 μL) were taken from the reaction mixture with a syringe. After completion of the injection, the heating mantle was removed and the solution was quickly cooled down to room temperature. The core/crown NPLs were collected by addition of a 2 : 1 ethanol : hexane mixture, followed by centrifugation (4226 rcf, 10 min). The NPLs were re-dispersed in 4 mL of hexane and stored under ambient conditions.

Table 1 Reaction parameters of CdS crown growth reactions leading to CdSe/CdS NPLs shown in Fig. 1(b)–(d). Tessier *et al.*[21] injected a gel-like mixture of oleic acid and cadmium and sulphur precursors at high temperatures. In the two other protocols, only the sulphur precursor was slowly injected while the cadmium precursor was added to the reaction flask before degassing

Precursor type		Precursor addition temperature (°C)		
Cd precursor	S precursor	Cd precursor	S precursor	Reference
$Cd(Ac)_2$	SODE premixed	240	240	21
$Cd(Ac)_2$	SODE	RT	240	43
$Cd(Ac)_2$	TOPS/ODE	RT	240	This work

In addition to the described protocol, two literature procedures were applied for the CdS crown growth.[21,43] The reaction parameters of all three protocols are compared in Table 1.

2.3 Characterisation techniques

2.3.1 UV/vis spectroscopy. UV/vis absorbance spectra were recorded with a Horiba Dual-FL spectrometer. All samples were diluted with hexane and measured in quartz cuvettes with a path length of 1 cm. For the measurement of UV/vis absorption spectra, an Agilent Cary 5000 UV-Vis-NIR spectrophotometer equipped with an Agilent DRA-2500 integrating sphere was applied. All spectra were recorded in the centre-mount position of the integrating sphere.

2.3.2 Photoluminescence spectroscopy. Photoluminescence (PL) emission and excitation spectra were measured with a Horiba Dual-FL spectrometer. PL quantum yields (PLQYs) were obtained in absolute mode with the same spectrometer equipped with a Quanta-Phi integrating sphere. It needs to be noted, that the presented PLQY measurements are not re-absorption corrected. Due to the strong overlap of the absorbance and emission spectrum for most of the samples, the reported PLQYs will be slightly lower than the true values. However, in order to minimise the resulting error very diluted samples were applied.

PL lifetime measurements were carried out at a FluoroMax-4 spectrometer from Horiba equipped with a FluoroHub time-correlated single photon counting (TCSPC) unit. The samples were excited with a $\lambda = 454$ nm pulsed LED light source. In all cases, the samples were diluted with hexane and measured in quartz cuvettes with a path length of 1 cm.

2.3.3 Atomic absorption spectroscopy. Atomic absorption spectroscopy (AAS) was applied to determine the Cd ion concentrations of the CdSe core NPL solutions. Therefore, a small known amount (typically 3 μL to 10 μL) of the NPL solution was digested with *aqua regia* over night. Afterwards, the solutions were transferred into 50 mL measurement flasks and filled with Milli-Q water ($R = 18.2$ MΩ cm). To obtain a calibration curve, at least 5 standard solutions in the concentration range between 0 ppm and 1.5 ppm were analysed. All measurements were carried out on a Varian AA140 instrument equipped with an air/acetylene (1.5 : 3.5) flame atomiser.

2.3.4 Transmission electron microscopy. For transmission electron microscopy (TEM) imaging, a FEI Tecnai G2 F20 equipped with a field emission gun working at an acceleration voltage of 200 kV was applied. The samples were prepared by drop-casting of 10 μL of a diluted NPL solution onto carbon-coated Cu grids (Quantifoil, 300 mesh).

2.3.5 Powder X-ray diffraction. Powder X-ray diffractograms (PXRDs) were recorded with a Bruker D8ADVANCE in reflection mode (Bragg–Brentano geometry). The samples were prepared by drop-casting concentrated solutions onto silicon single crystal sample carriers and subsequent drying under ambient conditions. Prior to the application onto the sample carrier, the NPL solutions were purified once using ethanol as the destabilisation agent.

3 Results and discussion

CdSe core NPLs with two different thicknesses (4 or 5 MLs), different lateral dimensions and different shapes (quasi-quadratic or quasi-rectangular) were synthesised according to slightly modified literature procedures.[10,22,25,32,41,42] The results of the optical and structural characterisation of the core NPLs are summarised in the ESI (Fig. S1–S4†).

Initially, quasi-quadratic NPLs (for characterisation see ESI Fig. S3†) were laterally extended with a CdS crown without changing their thickness [Fig. 1(a)]. Therefore, we applied two already published protocols[21,43] as well as a new one inspired by the procedure for CdTe (CdSe) growth on CdSe NPLs.[32] In the procedure introduced by Tessier *et al.*,[21] a pre-prepared mixture of oleic acid, cadmium acetate and sulphur in ODE is injected at a fixed rate into a solution of the CdSe core NPLs in ODE at the reaction temperature. Meerbach *et al.*,[43] in contrast, added a S/ODE solution at a slow injection rate whereas cadmium acetate and oleic acid were present in the reaction flask. Our new protocol is similar to the latter one, with the difference, that TOPS/ODE instead of S/ODE was applied as the sulphur precursor. More details on the synthesis parameters of the different methods are collected in Table 1. As can be seen in the TEM images of the synthesised CdSe/CdS NPLs [Fig. 1(b)–(d)], the shape and PLQY of the obtained core/crown NPLs strongly depends on the applied protocol.

Briefly, the addition of the Cd precursor before reaching the reaction temperature [as in Fig. 1(c) and (d)] and the application of TOPS as the sulphur precursor [as in Fig. 1(d)] seem to enhance the PLQY while also leading to a more regularly shaped CdS crown. The first-mentioned modification is likely limiting the destruction/etching of the core NPLs during the heat-up process, as it was already shown that, in the absence of cadmium carboxylates, CdSe NPLs start to dissolve if heated to temperatures above 210 °C to 240 °C.[28] The effect of the second modification, specifically the replacement of the standard sulphur precursor S/ODE by TOPS/ODE, will be explained shortly. Fig. 1(e) moreover shows the typical optical spectra of CdSe/CdS core/crown NPLs. While the absorption maxima of CdSe core NPLs, located at 511 nm and 480 nm, are observed to only shift negligibly (to 513 nm and 479 nm, respectively) during the crown growth, a distinct feature corresponding to the absorption of the CdS crown arises at $\lambda = 405$ nm. Due to the high exciton binding energy in Cd chalcogenide NPLs, the

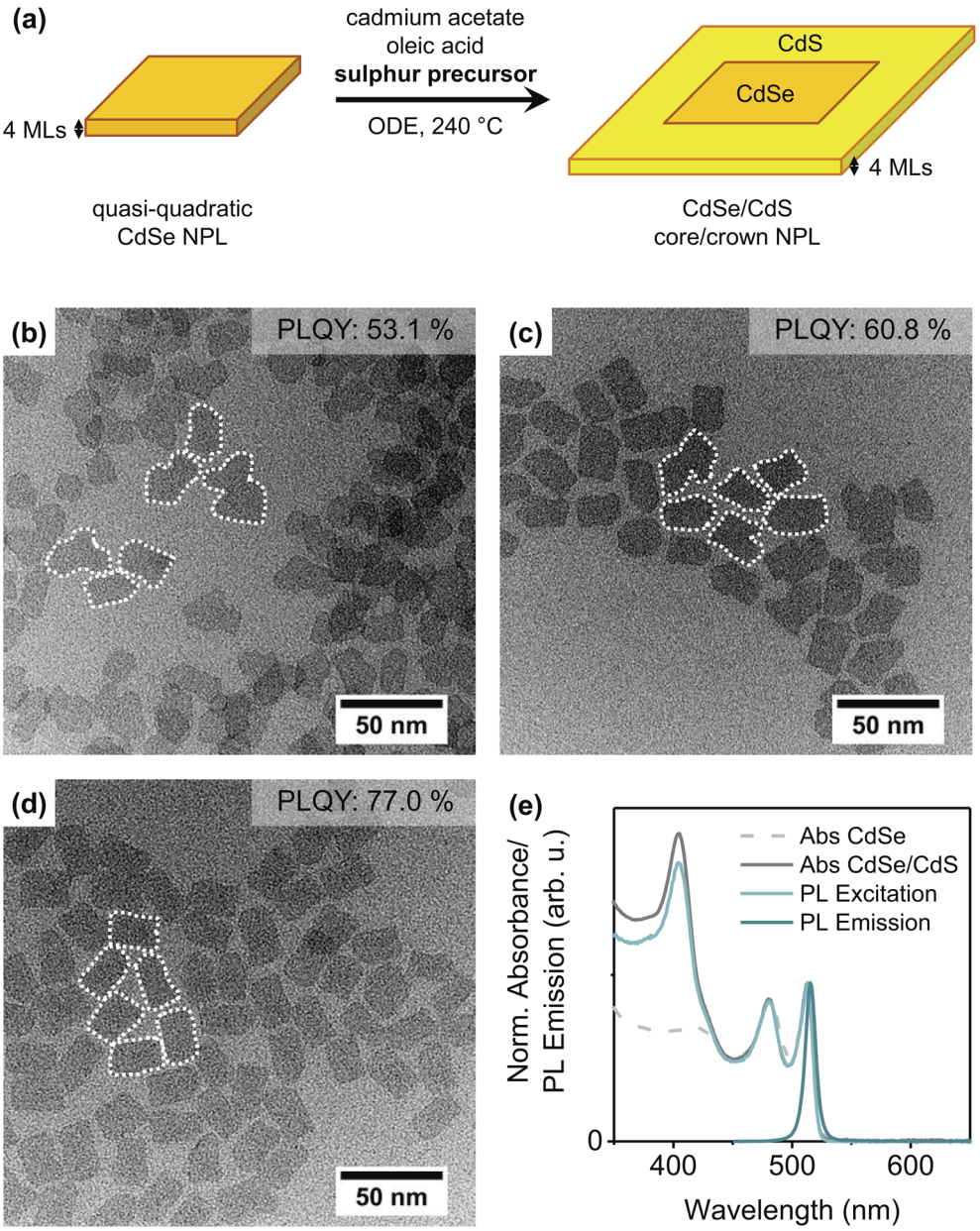

Fig. 1 (a) Schematic illustration of the CdS crown growth on quasi-quadratic 4 ML thick CdSe NPLs. (b)–(d) TEM images of CdSe/CdS core/crown NPLs synthesised by different protocols: (b) Tessier *et al.*,[21] (c) Meerbach *et al.*[43] (with slight modifications), (d) new protocol. Details on the different protocols are collected in Table 1. The white dotted lines were inserted to visualise the shape of the NPLs. (e) Normalised absorbance spectra of quasi-quadratic CdSe core NPLs (light grey, dashed) and CdSe/CdS core/crown NPLs (new protocol, dark grey), PL excitation (light blue) and PL emission spectra (dark blue) of CdSe/CdS NPLs.

radiative recombination takes place solely in the core of CdSe/CdS core/crown NPLs,[21,44] so only a slight bathochromic shift of the emission maximum of 2 nm and short PL lifetimes below 5 ns were recorded. The quantum yield of the CdSe NPLs increases dramatically during crown growth from below 1% for the bare CdSe NPLs to up to 80% for the core/crown NPLs. However, as mentioned previously, comparably high PLQYs can only be reached if TOP is present in the reaction mixture during the crown growth process.

To better understand the role of TOP in this reaction, we performed a series of experiments with different sulphur precursors (S/ODE and TOPS/ODE) and, in case of S/ODE, different amounts of TOP directly added to the reaction solution. The progress of the crown growth process could be monitored by taking aliquots of the reaction solution, which were purified and subsequently analysed by UV/vis and PL spectroscopy. Fig. 2(a) illustrates the development of the absorbance of CdSe/CdS core/crown NPLs during a crown growth reaction (S/ODE + 50 μL TOP). The maximum at around $\lambda = 405$ nm corresponding to the CdS crown absorption increases with progressing reaction and its relative absorbance value [obtained from absorbance spectra normalised to the

heavy hole-electron (hh-e) maximum of CdSe NPLs] can therefore be applied as a measure for the size of the CdS crown [Fig. 2(c) and ESI† section 2]. In Fig. 2(b) the relative absorbance at the CdS maximum was plotted against the reaction time for different sulphur precursor compositions. It is clearly visible, that the growth rate is remarkably higher if no or only a small amount of TOP is present.

In general, TOP can influence the NC (shell) growth in different ways which are all related to the high phosphorous-chalcogenide affinity: (1) TOP acts as a surface ligand preferably binding to chalcogenide-rich facets,[45–47] (2) TOP is able to activate CdX (X = S, Se, Te) NC surfaces by dissolving excess chalcogenides,[48] and (3) alkyl phosphines can reduce the reactivity of especially sulphur precursors due to the formation of strong P–S bonds.[49] To evaluate the influence of factors (1) and (2), the specific structure of zinc blende CdSe NPLs needs to be taken into account. It was shown, that both of the surfaces perpendicular to the NPL thickness direction are Cd-rich (100) planes, whereas the surfaces at the NPL edges contain equal amounts of Cd^{2+} and Se^{2-} ions.[50,51] Consequently, TOP molecules will rather bind to the NPL edges than to the top and bottom facets of the NPLs and could therefore slow down the lateral extension of the NPLs (*i.e.* the crown growth). However, due to the fact that the crown growth is sulphur-limited under the applied conditions, the reactivity of the sulphur precursor [factor (3)] might influence the growth rate even more strongly than both of the afore-mentioned effects. In case of S/ODE the reactivity of the sulphur precursor is high, so that the reaction is mainly limited by the availability of the sulphur precursor, *e.g.* the injection rate [Fig. 2 and ESI Fig. S6†]. In contrast, the TOPS based precursor (containing 300 μL of TOP in total) is less reactive and the reaction therefore proceeds at a reduced rate. This thermodynamic reaction control can also be achieved by adding at least 300 μL of TOP directly to the reaction solution while using S/ODE as the sulphur source. If only 150 μL of TOP are added, however, the reaction proceeds at an intermediate rate. This implies, that a certain excess of TOP in the reaction solution is required in order to achieve a complete *in situ*-complexation of the added sulphur. For the complete conversion of the applied sulphur to TOPS, only 134 μL of TOP would be required (assuming a complete and stoichiometric reaction). As can be seen in Fig. 2(c), the TOP amount, or more specifically the growth rate, also affects the PLQY of the synthesised CdSe/CdS core/crown NPLs. For TOP amounts of 150 μL or more, the

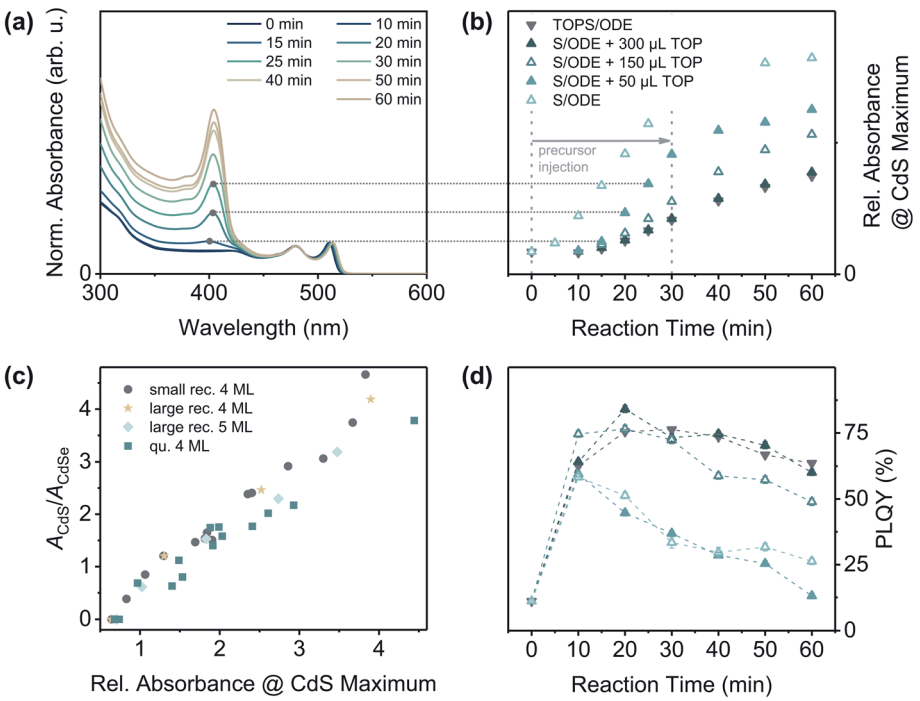

Fig. 2 (a) Normalised absorbance spectra of CdSe/CdS NPLs during a CdS crown growth reaction (here: quasi-quadratic CdSe cores + S/ODE + 50 μL TOP). The absorbance spectra were normalised to the absorbance maximum corresponding to the heavy hole–electron (hh–e) transition at around $\lambda = 511$ nm. In the first 30 min of the reaction, the sulphur precursor solution was injected at a rate of 12 mL h^{-1}. Afterwards, the reaction mixture was kept at 240 °C for another 30 min. (b) Progress of CdS crown growth reactions with different precursor compositions. Additional TOP was injected into the reaction flask directly before the addition of the S/ODE solution. The horizontal lines (medium grey dotted) were inserted to visualise how the *y*-coordinates of the data points in (b) were determined. In case of the reaction without TOP (S/ODE), the samples taken after 30 min and 40 min reaction time could reproducibly not be stabilised, so no absorbance values could be determined. (c) The relative absorbance at the CdS maximum [*y*-coordinate in (b)] is in good approximation linear to the area of the CdS crown, if the area of the CdSe core remains constant (for more details see ESI† Section 2). It can therefore be applied as measure for the reaction progress. The areas of the core (A_{CdSe}) and crown (A_{CdS}) were obtained from TEM measurements, the relative absorbance values were derived from the normalised absorbance spectra. (d) PLQY of the CdSe/CdS NPLs at different reaction stages (excitation wavelength: 460 nm). The dashed lines between the data points were inserted to facilitate the differentiation of the data sets. The key (symbols and colours) is the same as in (b).

PLQY initially increases until a certain crown size is reached (approx. 3–5 nm of shell material on each edge) and finally decreases to a value between 50 and 60%. Lower amounts of TOP (higher reaction rates) yield in CdSe/CdS NPLs with comparably lower PLQYs, even if the CdS area is similar in both cases. A similar relation between shell growth rate and PLQY was recently demonstrated for the ZnS shell growth on ZnSe nanorods.[36] In summary, it was demonstrated that replacing the common sulphur precursor for the CdS crown growth by a less reactive one allows the uniform growth of CdS crowns around quasi-quadratic CdSe NPLs, so that the PLQYs of the resulting core/crown NPLs can reach up to 80%. In addition to its effects on the sulphur reactivity, TOP presumably also acts as a tight-binding ligand which leads to a further reduction of the CdS growth rate.

To evaluate, if the availability of the sulphur precursor also influences the reaction outcome, we varied the injection rate of the TOPS/ODE solution. In addition to the injection at the 'standard' rate of 12 mL h^{-1}, the sulphur precursor was injected at rates of 6 mL h^{-1} and 36 mL h^{-1}, respectively. For both other injection rates, the reaction outcome was similar, but significantly different from the outcome of a reaction at the intermediate rate of 12 mL h^{-1}. The optical characterisation of CdSe/CdS NPLs synthesised with an injection rate of 6 mL h^{-1} is shown in Fig. 3(a) and (b). The growth of the CdS crown is again reflected in the increasing absorbance at around 405 nm [Fig. 3(a)]. In addition, a barely noticeable increase in absorbance at longer wavelengths (right green circle) than the hh-e absorbance maximum of 4 ML CdSe NPLs is appearing and intensifying over the course of the reaction. The impact of the lower injection rate onto the emission properties of the core/crown NPLs, however, is much more distinct. As can be seen in Fig. 3(b), a second broader emission peak at longer wavelengths appears and becomes more intense during the CdS growth, whereas the original sharp emission maximum at around 515 nm slowly decreases in intensity.

To identify, if both emission peaks originate from the same emitting species, we recorded PL excitation spectra at different emission wavelengths [Fig. 3(d)]. The excitation spectrum recorded at 516 nm [Fig. 3(d), dark grey solid line] resembles in principle the excitation spectrum of a comparable CdSe/CdS core/crown NPL solution with a single emission peak at 516 nm [Fig. 3(d), light grey dashed line], with a noticeable difference in the wavelength regime between 425 and 475 nm. We attribute this difference to the growth of a CdS crown, which is in part slightly thicker than 4 MLs, as this will result in additional light absorption at higher wavelengths than 405 nm.[21,43] The original emission wavelength, however, will remain nearly unchanged in this case, as the thickness of the CdSe core does not change and the conduction band offset between CdSe and CdS is still comparably small, so that the exciton binding energy cannot be overcome.[44] It needs to be noted, that under the applied reaction conditions the formation of a complete CdS layer on the top and bottom facets of the core NPLs is generally unlikely, as it requires higher reaction temperatures and/or an excess of the chalcogenide precursor.[16,23,28,52,53]

In addition to this first population of NPLs, a second NPL population with an even thicker CdS crown and a bathochromically shifted emission seems to be present. The excitation spectra recorded at this emission peak [Fig. 3(d) blue shaded lines] reveal, that the absorbance feature at higher wavelengths is solely originating from this second class of NPLs. It can moreover be noticed, that the features corresponding to the CdSe core NPLs are still comparatively sharp and only negligibly shifted to higher wavelengths. This leads to the conclusion, that the core is still intact and its thickness remains mostly constant, as already the formation of an incomplete monolayer of sulfide on the top and bottom facets of CdSe NPLs would lead to a remarkable broadening of the absorbance maxima and a shift to higher wavelengths of at least 20 nm.[20,52–54] Hence, the bathochromic shift in the emission might originate from the change from core-only to interface-dominated emission as the thickness of the CdS crown and therewith the conduction band offset between CdSe and CdS increases (partial delocalisation of the excited electron into the crown). This assumption is further corroborated by the higher PL lifetime of NPLs with a bathochromically shifted emission [shorter components of 3.5 ns and 10.1 ns for populations emitting at 516 nm and 558 nm, respectively, for more details see ESI Fig. S15(a) and Table S2†]. However, it can still not be fully excluded that a small amount of CdS also grows onto the CdSe core, as this would also lead to a bathochromic emission shift and a prolonged PL lifetime. Additionally, the previously described structural changes are confirmed by the TEM characterisation results [Fig. 3(e) and (f)]. In particular, regions with a higher contrast close to the edges and corners of some of the NPLs (white circles) are visible in the TEM image of CdSe/CdS NPLs synthesised with a lower injection rate [Fig. 3(e)]. This suggests a higher material thickness in these regions, as there are no noticeable contrast differences for CdSe/CdS core/crown NPLs with a uniform thickness [Fig. 3(f)]. In addition, NPLs synthesised at the lower injection rate are characterised by a more random shape without straight edges. If the CdS growth proceeds further, the amount of CdS grown onto the top and bottom facets of the NPLs increases but no homogeneous ring of CdS on the crown edges is formed (ESI Fig. S12†). Instead, a sole 2D extension of the crown is observed for some edges. Thus, the 3D growth seems to be favoured over 2D growth only on specific edges, probably on those which are characterised by a comparatively higher TOP coverage.

In addition to the blocking of some edge facets by TOP, the amount of acetate present in the synthesis mixture might be one of the crucial factors for the change in the growth dimensionality from 2D to 3D. Short carboxylates were previously identified as one of the primary keys to the 2D growth of cadmium chalcogenide NPLs.[21,31] In the presented synthesis procedure, cadmium acetate dihydrate is applied as the cadmium precursor, however, a considerable amount of acetic acid is likely already removed during the degassing process in vacuum. Additionally, cadmium carboxylates were demonstrated to be able to react with phosphine chalcogenides forming Lewis acid–base adducts.[55] This, in turn, might lead to a further reduction of the amount of free acetate in the reaction

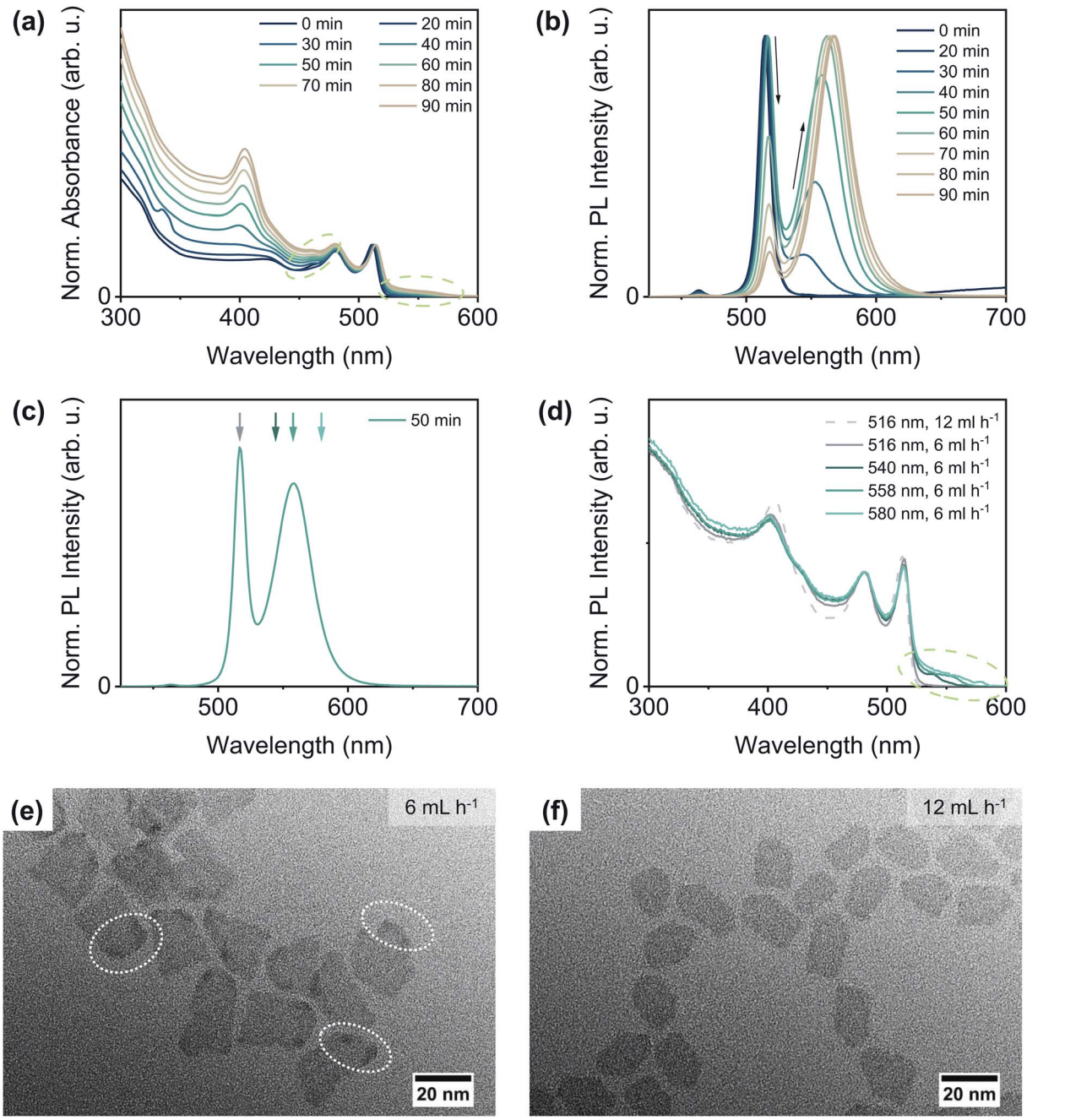

Fig. 3 Characterisation results of CdSe/CdS core/crown NPLs synthesised from quasi-quadratic CdSe NPLs at a TOPS/ODE injection rate of 6 mL h^{-1}. Time-dependent normalised (a) absorbance and (b) PL emission spectra. The absorbance spectra were normalised to the hh–e absorbance maximum, the PL emission spectra to the wavelength, at which the highest PL emission intensity was recorded. Further optical characterisation results (*e.g.* absorption spectra, PLQYs, PL lifetimes) are shown in the ESI† in Section 4. (c) PL emission spectrum after 50 min reaction time extracted from (b) to demonstrate at which emission wavelengths the different PL excitation spectra in (d) were recorded. (e) + (f) TEM images of CdSe/CdS NPLs synthesised with injection rates of (e) 6 mL h^{-1} and (f) 12 mL h^{-1} after (e) 50 min and (f) 25 min reaction time (corresponding to injection of 5 mL of TOPS/ODE).

mixture and could moreover alter the reaction pathway (especially the reaction intermediates). Hence, the reduced availability of acetate is probably another important factor for the observed increase in the crown thickness.

As it was stated beforehand, thick-crown CdSe/CdS NPLs also form at very high injection rates. Detailed results of this synthesis as well as additional characterisation of thick-crown CdSe/CdS NPLs are available in the ESI† (Section 4). Under these conditions, the thickening process of the crown could be related to a combination of a high (sulphur) precursor concentration and the inactivation of the edge surfaces by TOP molecules. Directly after its formation, the surface of the CdS crown might not be completely defect-free and not yet fully covered with oleate ligands. Thus, the formation of a thicker

CdS crown could be energetically favoured compared to further lateral extension *via* the edge facets. Higher injection rates could moreover lead to increased homogeneous (secondary) nucleation.[21,56] However, neither in the TEM images, nor in any optical spectra there was any evidence for the presence of CdS NCs, which is possibly another benefit of the low reactivity of the applied sulphur precursor. In summary, the structural and optical properties of CdSe/CdS core/crown NPLs synthesised from quasi-quadratic core NPLs depend strongly on the injection rate, if TOPS is applied as the sulphur precursor. A sole two-dimensional extension of the core is only achieved at an intermediate injection rate of 12 mL h^{-1}, whereas higher and lower rates lead to the formation of a CdS crown with a thickness of partially more than 4 MLs.

In order to investigate whether similar effects are also observed for CdSe NPLs with other geometries, we applied quasi-rectangular 4 ML CdSe NPLs with a comparable NPL area to that of the quasi-quadratic NPLs (for characterisation see ESI Fig. S1†) as seeds for the CdS crown growth. In Fig. 4(a) the crown growth rates at different sulphur precursor injection rates (6, 12 and 36 mL h^{-1}) are shown. At none of the applied injection rates, a similar thickening of the CdS crown as in case of the quasi-quadratic NPLs was registered. Related to the total reaction time, the crown growth rate was observed to increase with the injection rate. This observation may be explained by the different end points of the precursor injection [Fig. 4(a), framed data points] and the therefore large differences of the sulphur precursor concentration, especially at the beginning of the reactions. The sulphur precursor concentration moreover affects the length of the induction period, which was found to increase with decreasing injection rate.

A comparison of the CdS crown growth rates of NPLs with different core geometries reveals, that the CdS growth proceeds faster on NPLs with a quasi-rectangular shape. Primarily, this effect could have been induced by the lower total edge length of a square in relation to a rectangle with the same area. Considering the tendency of quasi-quadratic core NPLs to form CdS crowns with a higher thickness than the core, the lower lateral growth rate is probably also a result of the comparably stronger binding of TOP molecules to the edge facets of quasi-quadratic NPLs. This, however, might correlate with the following points: (1) a higher selenium content of the edge facets, (2) the presence of edge facets which allow the formation of TOP–Se bonds in a favoured bond angle and (3) a lower coverage with native ligands in case of quasi-quadratic CdSe NPLs. The latter is confirmed by the significantly lower PLQY of quasi-quadratic core only NPLs after purification (0.7% *vs.* 8.0% for quasi-rectangular NPLs).[33,57] In this regard, also the differences in the formation process of NPLs with different aspect ratios need to be taken into account. While the thickness of CdSe NPLs is kinetically controlled,[58,59] their shape (in case of 4 ML NPLs) is determined by the amount of water (more precisely the amount of OH^- ions) in the reaction mixture.[60] To obtain NPLs with low aspect ratios (*i.e.* quasi-quadratic NPLs), for example, high amounts of OH^- ions are required. If a significant number of these ions remains on the surface of the NPLs after the purification steps, further modifications (*e.g.* the crown growth) might also be influenced. The released OH^- ions could interfere with the CdS crown growth especially at high relative concentrations in comparison to the precursor anions, which is *e.g.* the case at low injection rates. In summary, two different effects could be responsible for the observed differences in the CdS crown growth on core NPLs with different geometries: (1) different amounts of TOP bound to the edge facets of the NPLs and (2) release of OH^- ions during the reaction.

In addition to the crown growth rates, the PLQYs at similar crown sizes were compared for the different reaction conditions and core geometries [Fig. 4(b)]. In general, CdSe/CdS core/crown NPLs synthesised from quasi-quadratic cores were observed to exhibit lower PLQYs than their counterparts

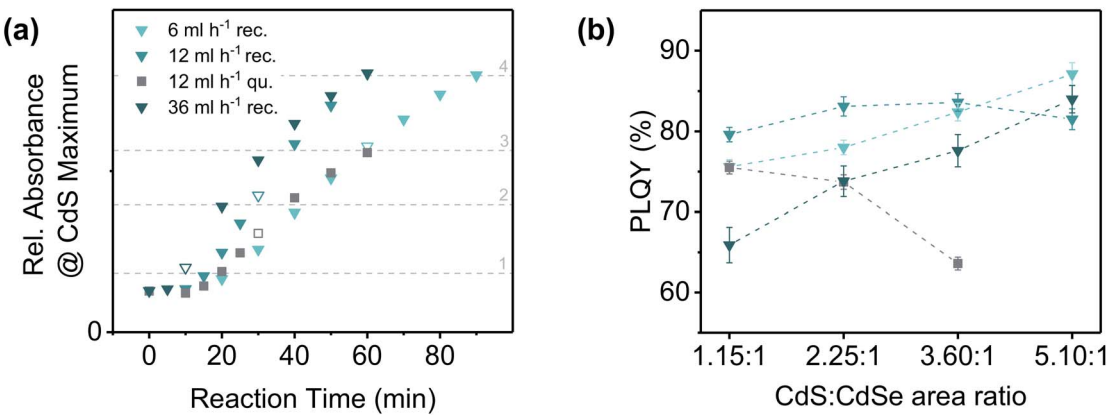

Fig. 4 (a) Progress of CdS crown growth on quasi-rectangular (blue shaded triangles) and quasi-quadratic (dark grey squares) CdSe NPLs. The points, at which the whole precursor amount was added to the reaction solution are symbolised by white triangles or squares framed in the colour of the respective series. The absorbance of quasi-quadratic NPLs was corrected with a response factor in order to take account of the differences in the absorbance-CdS area relation in case of different core geometries (for details see ESI Table S1†). (b) Comparison of the PLQYs (excitation wavelength: 460 nm) of CdSe/CdS core/crown NPLs with similar CdS crown sizes synthesised with different precursor injection rates. Approximate CdS : CdSe area ratios: (1) 1.15 : 1, (2) 2.25 : 1, (3) 3.60 : 1, (4) 5.10 : 1. The relative absorbance values appertaining to the respective crown areas are symbolised by light grey horizontal lines [in (a)]. The key (symbols and colours) is the same as in (a). The dashed lines between the data points were inserted to facilitate the differentiation of the data sets.

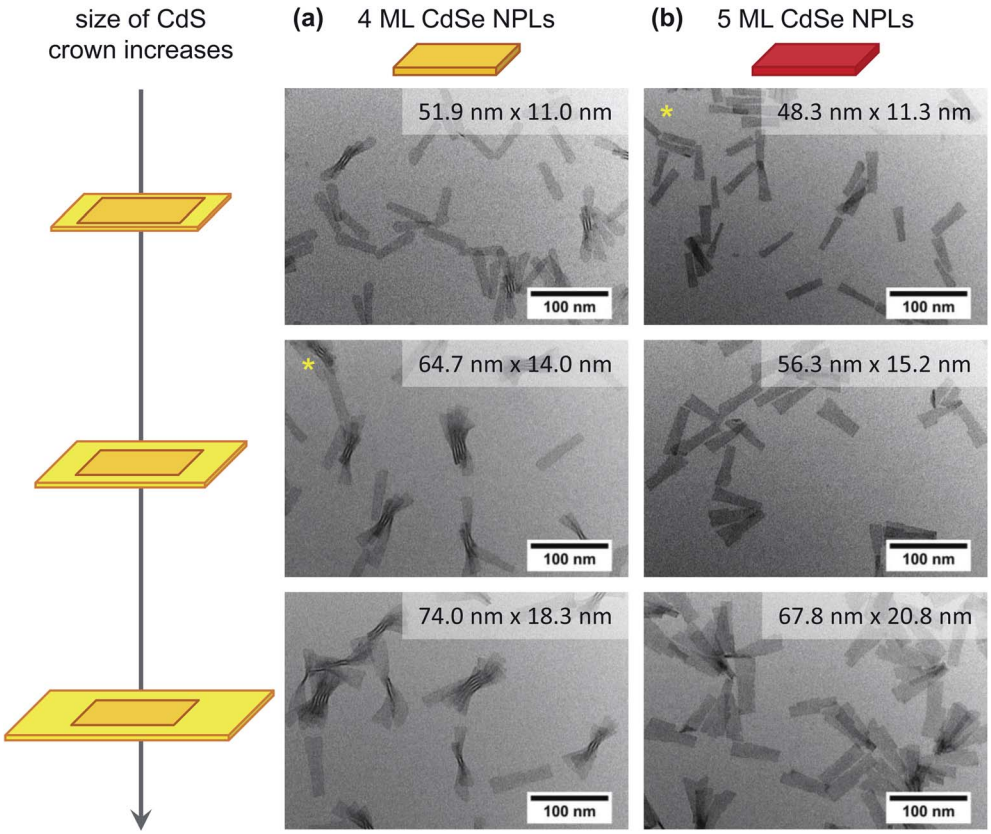

Fig. 5 Evolution of the NPL shape and size during CdS crown growth on (a) quasi-rectangular 4 ML NPLs (36.1 nm × 7.3 nm × 1.2 nm) and (b) quasi-rectangular 5 ML NPLs (37.3 nm × 9.0 nm × 1.5 nm). The average values for the length and width of the core/crown NPLs are displayed in the top right corners of the TEM images. The samples with the highest PLQY of the respective series are marked with a yellow asterisk. The aspect ratios (length divided by width) of the NPLs were observed to decrease due to the crown growth: in case of 4 ML NPLs from 5.2 ± 1.2 to 4.1 ± 0.5 (core NPLs *vs.* largest core/crown NPLs) and in case of 5 ML NPLs from 4.4 ± 1.2 to 3.3 ± 0.4.

originating from quasi-rectangular cores. The only exception was formed by the smallest core/crown NPLs synthesised at an injection rate of 36 mL h^{-1}. As mentioned before, high injection rates result in a comparable fast growth of the crown which might lead to a higher defect density and an incomplete ligand coverage of the crown and therewith lower PLQYs. It was moreover observed, that the PLQY of CdSe/CdS NPLs with a quasi-quadratic core decreases with an increasing crown size, whereas it increases for CdSe/CdS NPLs with a quasi-rectangular core. However, for larger quasi-rectangular 4 ML NPLs as well as 5 ML NPLs a different relation between PLQYs and crown area was obtained [ESI Fig. S21(b)†]. The PLQY of those core NPLs was observed to increase until a certain crown size was reached and to subsequently decrease again. For the largest applied core NPLs (5 ML quasi-rectangular), this turning point was located at even lower CdS crown sizes, which leads to the conclusion, that there might be a correlation between the total NPL area and the PLQY. In the TEM images of CdSe/CdS large core/crown (4 ML and 5 ML) NPLs (Fig. 5) it can be noticed, that the shape of the NPLs becomes more irregular with increasing crown size. Especially in case of the largest 5 ML CdSe/CdS NPLs, dislocations at the NPL edges are visible so that the width of the NPL is inconstant over its length. For core/crown NPLs originating from 4 ML cores [Fig. 5(a)], similar inconsistencies, but nearly no dislocations were observed. At the earliest shown stage of the reaction [Fig. 5(a) top], the crown moreover appears to be slightly rounded at one of the shorter edges. A similar effect was observed in case of CdSe/CdS core/crown NPLs originating from smaller 4 ML core NPLs (ESI Fig. S20†). In summary, the PLQY of CdSe/CdS core/crown NPLs synthesised from quasi-rectangular cores mainly depends on the uniformity of the CdS crown. Lower PLQYs were recorded for core/crown NPLs with rounded corners as well as for core/crown NPLs with visible dislocations in the crown edges.

4 Conclusions

We have presented an improved protocol for the synthesis of CdSe/CdS core/crown nanoplatelets (NPLs) with high photoluminescence quantum yields (PLQYs) starting from a variety of CdSe NPL core geometries and thicknesses. In the new protocol, tri-*n*-octylphosphine (TOP) was applied to slow down the crown growth in order to achieve crowns with an increased uniformity and therefore higher PLQYs. In case of quasi-quadratic core NPLs, the injection rate needed to be tuned very precisely to avoid the formation of CdS crowns with a partially higher thickness than the CdSe core. For core/crown

NPLs based on quasi-rectangular cores, however, no similar effects were observed, which was attributed to a comparably higher reactivity of the edge facets in the presence of TOP and a lower amount of residual OH^- ions.

In summary, the new synthesis protocol is characterised by a very good reproducibility, can be easily scaled up and yields extremely stable NPL dispersions and might therefore promote the application of CdSe/CdS core/crown NPLs in the fields of optoelectronics, photocatalysis and photoelectrochemistry.

Conflicts of interest

There are no conflicts to declare.

Acknowledgements

The authors are grateful for financial support from the German Federal Ministry of Education and Research (BMBF) within the framework of the program NanoMatFutur, support code 03X5525. In addition, the project leading to these results has in part received funding from the European Research Council (ERC) under the European Union's Horizon 2020 research and innovation program (grant agreement No. 714429). Furthermore, the project has in parts been funded by the Deutsche Forschungsgemeinschaft (DFG, German Research Foundation) under Germany's Excellence Strategy within the Cluster of Excellence PhoenixD (EXC 2122, project ID 390833453). N. C. B. moreover acknowledges the DFG (grant agreement BI 1708/4-1) for funding. A. S. and R. T. G. would like to thank the Hannover School for Nanotechnology (HSN) for financial support. The authors would moreover like to acknowledge Armin Feldhoff as well as Jürgen Caro for providing the XRD facilities.

References

1 S. Ithurria and B. Dubertret, *J. Am. Chem. Soc.*, 2008, **130**, 16504–16505.
2 M. Nasilowski, B. Mahler, E. Lhuillier, S. Ithurria and B. Dubertret, *Chem. Rev.*, 2016, **116**, 10934–10982.
3 S. Ithurria, M. D. Tessier, B. Mahler, R. P. S. M. Lobo, B. Dubertret and A. L. Efros, *Nat. Mater.*, 2011, **10**, 936–941.
4 A. Yeltik, S. Delikanli, M. Olutas, Y. Kelestemur, B. Guzelturk and H. V. Demir, *J. Phys. Chem. C*, 2015, **119**, 26768–26775.
5 J. Q. Grim, S. Christodoulou, F. Di Stasio, R. Krahne, R. Cingolani, L. Manna and I. Moreels, *Nat. Nanotechnol.*, 2014, **9**, 891–895.
6 M. Li, M. Zhi, H. Zhu, W.-Y. Wu, Q.-H. Xu, M. H. Jhon and Y. Chan, *Nat. Commun.*, 2015, **6**, 8513.
7 C. She, I. Fedin, D. S. Dolzhnikov, A. Demortière, R. D. Schaller, M. Pelton and D. V. Talapin, *Nano Lett.*, 2014, **14**, 2772–2777.
8 B. Guzelturk, Y. Kelestemur, M. Olutas, S. Delikanli and H. V. Demir, *ACS Nano*, 2014, **8**, 6599–6605.
9 M. Lorenzon, S. Christodoulou, G. Vaccaro, J. Pedrini, F. Meinardi, I. Moreels and S. Brovelli, *Nat. Commun.*, 2015, **6**, 6434.
10 A. Schlosser, L. C. Meyer, F. Lübkemann, J. F. Miethe and N. C. Bigall, *Phys. Chem. Chem. Phys.*, 2019, **21**, 9002–9012.
11 Z. Chen, B. Nadal, B. Mahler, H. Aubin and B. Dubertret, *Adv. Funct. Mater.*, 2014, **24**, 295–302.
12 B. Liu, S. Delikanli, Y. Gao, D. Dede, K. Gungor and H. V. Demir, *Nano Energy*, 2018, **47**, 115–122.
13 U. Giovanella, M. Pasini, M. Lorenzon, F. Galeotti, C. Lucchi, F. Meinardi, S. Luzzati, B. Dubertret and S. Brovelli, *Nano Lett.*, 2018, **18**, 3441–3448.
14 F. Zhang, S. Wang, L. Wang, Q. Lin, H. Shen, W. Cao, C. Yang, H. Wang, L. Yu, Z. Du, J. Xue and L. S. Li, *Nanoscale*, 2016, **8**, 12182–12188.
15 Z. Wen, C. Zhang, Z. Zhou, B. Xu, K. Wang, K. L. Teo and X. W. Sun, *IEEE J. Quantum Electron.*, 2020, **56**, 1–6.
16 Y. Kelestemur, Y. Shynkarenko, M. Anni, S. Yakunin, M. L. De Giorgi and M. V. Kovalenko, *ACS Nano*, 2019, **13**, 13899–13909.
17 Z. Wen, F. Fang, C. Zhang, S. Ding, J. Sun, H. Tang, B. Xu, K. Wang, K. L. Teo and X. W. Sun, *J. Soc. Inf. Disp.*, 2019, **27**, 587–596.
18 E. Lhuillier, A. Robin, S. Ithurria, H. Aubin and B. Dubertret, *Nano Lett.*, 2014, **14**, 2715–2719.
19 T. K. Kormilina, S. A. Cherevkov, A. V. Fedorov and A. V. Baranov, *Small*, 2017, **13**, 1702300.
20 B. Mahler, B. Nadal, C. Bouet, G. Patriarche and B. Dubertret, *J. Am. Chem. Soc.*, 2012, **134**, 18591–18598.
21 M. D. Tessier, P. Spinicelli, D. Dupont, G. Patriarche, S. Ithurria and B. Dubertret, *Nano Lett.*, 2014, **14**, 207–213.
22 S. Pedetti, S. Ithurria, H. Heuclin, G. Patriarche and B. Dubertret, *J. Am. Chem. Soc.*, 2014, **136**, 16430–16438.
23 A. A. Rossinelli, H. Rojo, A. S. Mule, M. Aellen, A. Cocina, E. De Leo, R. Schäublin and D. J. Norris, *Chem. Mater.*, 2019, **31**, 9567–9578.
24 S. Yadav, B. Adhikary, P. Tripathy and S. Sapra, *ACS Omega*, 2017, **2**, 2231–2237.
25 S. Naskar, A. Schlosser, J. F. Miethe, F. Steinbach, A. Feldhoff and N. C. Bigall, *Chem. Mater.*, 2015, **27**, 3159–3166.
26 S. Naskar, F. Lübkemann, S. Hamid, A. Freytag, A. Wolf, J. Koch, I. Ivanova, H. Pfnür, D. Dorfs, D. W. Bahnemann and N. C. Bigall, *Adv. Funct. Mater.*, 2017, **27**, 1604685.
27 M. D. Tessier, B. Mahler, B. Nadal, H. Heuclin, S. Pedetti and B. Dubertret, *Nano Lett.*, 2013, **13**, 3321–3328.
28 A. A. Rossinelli, A. Riedinger, P. Marqués-Gallego, P. N. Knüsel, F. V. Antolinez and D. J. Norris, *Chem. Commun.*, 2017, **53**, 9938–9941.
29 A. Polovitsyn, Z. Dang, J. L. Movilla, B. Martín-García, A. H. Khan, G. H. V. Bertrand, R. Brescia and I. Moreels, *Chem. Mater.*, 2017, **29**, 5671–5680.
30 Y. Altintas, U. Quliyeva, K. Gungor, O. Erdem, Y. Kelestemur, E. Mutlugun, M. V. Kovalenko and H. V. Demir, *Small*, 2019, **15**, 1804854.
31 A. Prudnikau, A. Chuvilin and M. Artemyev, *J. Am. Chem. Soc.*, 2013, **135**, 14476–14479.
32 M. Dufour, V. Steinmetz, E. Izquierdo, T. Pons, N. Lequeux, E. Lhuillier, L. Legrand, M. Chamarro, T. Barisien and S. Ithurria, *J. Phys. Chem. C*, 2017, **121**, 24816–24823.

33 S. Singh, R. Tomar, S. Ten Brinck, J. De Roo, P. Geiregat, J. C. Martins, I. Infante and Z. Hens, *J. Am. Chem. Soc.*, 2018, **140**, 13292–13300.
34 J. Zhang, H. Zhang, W. Cao, Z. Pang, J. Li, Y. Shu, C. Zhu, X. Kong, L. Wang and X. Peng, *J. Am. Chem. Soc.*, 2019, **141**, 15675–15683.
35 O. Chen, J. Zhao, V. P. Chauhan, J. Cui, C. Wong, D. K. Harris, H. Wei, H.-S. Han, D. Fukumura, R. K. Jain and M. G. Bawendi, *Nat. Mater.*, 2013, **12**, 445–451.
36 B. Ji, S. Koley, I. Slobodkin, S. Remennik and U. Banin, *Nano Lett.*, 2020, **20**, 2387–2395.
37 T. Pons, N. Lequeux, B. Mahler, S. Sasnouski, A. Fragola and B. Dubertret, *Chem. Mater.*, 2009, **21**, 1418–1424.
38 Z. Li, X. Ma, Q. Sun, Z. Wang, J. Liu, Z. Zhu, S. Z. Qiao, S. C. Smith, G. M. Lu and A. Mews, *Eur. J. Inorg. Chem.*, 2010, **27**, 4325–4331.
39 B. Mahler, N. Lequeux and B. Dubertret, *J. Am. Chem. Soc.*, 2010, **132**, 953–959.
40 D. V. Talapin, J. H. Nelson, E. V. Shevchenko, S. Aloni, B. Sadtler and A. P. Alivisatos, *Nano Lett.*, 2007, **7**, 2951–2959.
41 B. Abécassis, M. D. Tessier, P. Davidson and B. Dubertret, *Nano Lett.*, 2014, **14**, 710–715.
42 J. F. Miethe, A. Schlosser, J. G. Eckert, F. Lübkemann and N. C. Bigall, *J. Mater. Chem. C*, 2018, **6**, 10916–10923.
43 C. Meerbach, C. Wu, S. C. Erwin, Z. Dang, A. Prudnikau and V. Lesnyak, *Chem. Mater.*, 2020, **32**, 566–574.
44 F. Rajadell, J. I. Climente and J. Planelles, *Phys. Rev. B*, 2017, **96**, 035307.
45 A. Puzder, A. J. Williamson, N. Zaitseva, G. Galli, L. Manna and A. P. Alivisatos, *Nano Lett.*, 2004, **4**, 2361–2365.
46 M. Green, *J. Mater. Chem.*, 2010, **20**, 5797–5809.
47 L. R. Becerra, C. B. Murray, R. G. Griffin and M. G. Bawendi, *J. Chem. Phys.*, 1994, **100**, 3297–3300.
48 J.-j. Hao, J. Zhou and C.-Y. Zhang, *Chem. Commun.*, 2013, **49**, 6346–6348.
49 L. A. Swafford, L. A. Weigand, M. J. Bowers, J. R. McBride, J. L. Rapaport, T. L. Watt, S. K. Dixit, L. C. Feldman and S. J. Rosenthal, *J. Am. Chem. Soc.*, 2006, **128**, 12299–12306.
50 S. J. Lim, W. Kim and S. K. Shin, *J. Am. Chem. Soc.*, 2012, **134**, 7576–7579.
51 Z. Li and X. Peng, *J. Am. Chem. Soc.*, 2011, **133**, 6578–6586.
52 C. Meerbach, R. Tietze, S. Voigt, V. Sayevich, V. M. Dzhagan, S. C. Erwin, Z. Dang, O. Selyshchev, K. Schneider, D. R. T. Zahn, V. Lesnyak and A. Eychmüller, *Adv. Opt. Mater.*, 2019, **7**, 1801478.
53 S. Ithurria and D. V. Talapin, *J. Am. Chem. Soc.*, 2012, **134**, 18585–18590.
54 S. Yadav, A. Singh, L. Thulasidharan and S. Sapra, *J. Phys. Chem. C*, 2018, **122**, 820–829.
55 R. García-Rodríguez, M. P. Hendricks, B. M. Cossairt, H. Liu and J. S. Owen, *Chem. Mater.*, 2013, **25**, 1233–1249.
56 S. Fischer, J. K. Swabeck and A. P. Alivisatos, *J. Am. Chem. Soc.*, 2017, **139**, 12325–12332.
57 C. Zhu, D. Chen, W. Cao, R. Lai, C. Pu, J. Li, X. Kong and X. Peng, *Angew. Chem., Int. Ed.*, 2019, **58**, 17764–17770.
58 A. Riedinger, F. D. Ott, A. Mule, S. Mazzotti, P. N. Knüsel, S. J. P. Kress, F. Prins, S. C. Erwin and D. J. Norris, *Nat. Mater.*, 2017, **16**, 743–748.
59 F. D. Ott, A. Riedinger, D. R. Ochsenbein, P. N. Knüsel, S. C. Erwin, M. Mazzotti and D. J. Norris, *Nano Lett.*, 2017, **17**, 6870–6877.
60 G. H. V. Bertrand, A. Polovitsyn, S. Christodoulou, A. H. Khan and I. Moreels, *Chem. Commun.*, 2016, **52**, 11975–11978.

